frontiers | Frontiers in Physics

TYPE Original Research
PUBLISHED 10 July 2025
DOI 10.3389/fphy.2025.1595410

OPEN ACCESS

EDITED BY
Qiuqin Sun,
Hunan University, China

REVIEWED BY
Bystrík Dolník,
Technical University of Košice, Slovakia
Yanhui Wei,
Qingdao University of Science and Technology, China
Anil Khopkar,
Electrical Research And Development Association (ERDA), India

*CORRESPONDENCE
Yongling Lu,
1395500274@qq.com

RECEIVED 18 March 2025
ACCEPTED 28 May 2025
PUBLISHED 10 July 2025

CITATION
Lu Y, Xue Z, Guo J, Zhang C, Liu J, Xiao X and Sun J (2025) Aging monitoring and fault positioning for zinc oxide surge arresters based on the fifth harmonic of the leakage current.
Front. Phys. 13:1595410.
doi: 10.3389/fphy.2025.1595410

Aging monitoring and fault positioning for zinc oxide surge arresters based on the fifth harmonic of the leakage current

Yongling Lu*, Zhitong Xue, Jiahao Guo, Chenyu Zhang, Jian Liu, Xiaolong Xiao and Jian Sun

State Grid Jiangsu Electric Power Research Institute Co., Ltd., Nanjing, Jiangsu, China

Current techniques for aging monitoring and fault positioning for zinc oxide surge arresters usually use the third harmonic of the leakage resistive current. However, harmonic interference in the power grid voltage greatly affects the third harmonic, resulting in poor monitoring and positioning effects. Therefore, based on the harmonic characteristics of the resistive current, this article adopts the fifth harmonic of the leakage current as a novel monitoring indicator for zinc oxide surge arresters. In addition, it builds an aging experimental platform for zinc oxide surge arresters with voltage harmonic interference. An improved displacement current method and a fast Fourier transform algorithm are used to extract current harmonic features, and the percentage changes in features and harmonic sensitivity are introduced to analyze the fifth harmonic characteristics. A monitoring threshold and positioning scheme is proposed. The results show that the fifth harmonic exhibits high sensitivity to faults, with smaller changes in harmonic sensitivity and characteristic percentage, stronger resistance to harmonic interference. Furthermore, it is more suitable for aging monitoring and fault positioning for zinc oxide surge arresters than existing third harmonic analysis methods.

KEYWORDS

leakage current, third harmonic of resistive current, fifth harmonic of the resistive current, aging monitoring and positioning zinc oxide surge arresters, aging monitoring and positioning

1 Introduction

Zinc oxide surge arresters are extensively used to protect electrical systems from transient overvoltage caused by severe lightning strikes and grid switching operations [1]. However, the aging of valve discs of arresters typically leads to increased conductivity. Moreover, in severe cases, internal flashovers and arrester explosions can severely disrupt the normal operation of zinc oxide surge arresters [2–5]. Arrester failure warrants immediate localization and replacement by operators to prevent interference with other electrical equipment in the grid [6]. Therefore, it is crucial to investigate aging monitoring and fault positioning for zinc oxide surge arresters.

Several methods, including residual voltage method [7], power loss measurement [8], leakage current measurement [9], capacitive current compensation [10], and harmonic analysis [11], have been proposed for monitoring the aging and fault conditions of zinc oxide surge arresters. Leakage current measurement is the most widely adopted for arrester

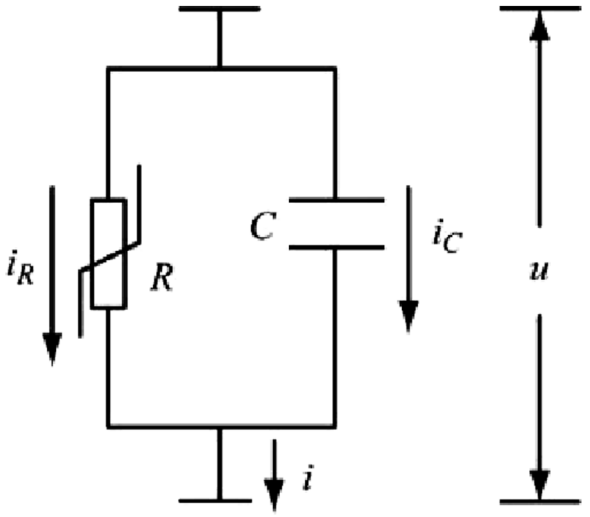

FIGURE 1
Equivalent circuit model of zinc oxide surge arresters.

condition assessment owing to its convenience and high accuracy [12]. Arrester failure can cause a significant surge in the total leakage current, exhibiting noticeable distortion in the waveform [13, 14]. The total leakage current is the vector sum of the resistive component i_R and the capacitive component i_C, as shown in Figure 1. The resistive leakage current is influenced by the applied voltage, fault characteristics, and ambient temperature. In addition, it exhibits high sensitivity to arrester faults and degradation [15, 16]. Since the variation in the third harmonic of the resistive current is more pronounced than that of the fundamental wave, it can be used for diagnosing arrester fault conditions [17]. However, the third harmonic of the resistive current is also affected by harmonics in the grid voltage, especially the third harmonic of the voltage, which significantly impacts the third harmonic of the resistive current [18, 19]. This interference prevents the precise reflection of arrester fault conditions. Therefore, a new monitoring indicator that is robust against voltage harmonic interference is necessary.

Recently, Wang et al. [20] from the China Electric Power Research Institute investigated the variation trends in resistive current and harmonics under system voltage harmonics, particularly noting the significant effect it had on the third harmonic, and proposed an integrated online monitoring device for arresters. Qi et al. [21] from Wuhan University of Technology proposed a waveform distortion correction method based on measured voltage waveforms to eliminate the effect of high-order voltage harmonics on resistive current and identified the true value of the leakage current. Additionally, Khodsuz and Mirzaie [22] from Brno University of Technology proposed a technique for eliminating the effect of voltage third harmonics on the resistive leakage current based on grid voltage analysis. However, these studies rely on measuring grid voltage harmonics, which not only increases the measurement and computational burden but also is not conducive to the reliability and effectiveness of fault monitoring and positioning for online arresters.

To address these challenges, this study proposes the fifth harmonic of the resistive leakage current as a new indicator for aging monitoring and fault positioning for zinc oxide surge arresters. First, an aging experimental platform was established for zinc oxide surge arresters, with harmonic components added to the applied voltage to simulate grid voltage harmonic interference. Second, the resistive leakage current was extracted using an improved displacement current method, and the harmonic components of the resistive current were determined using the fast Fourier transform (FFT) algorithm. Finally, the variations in characteristic

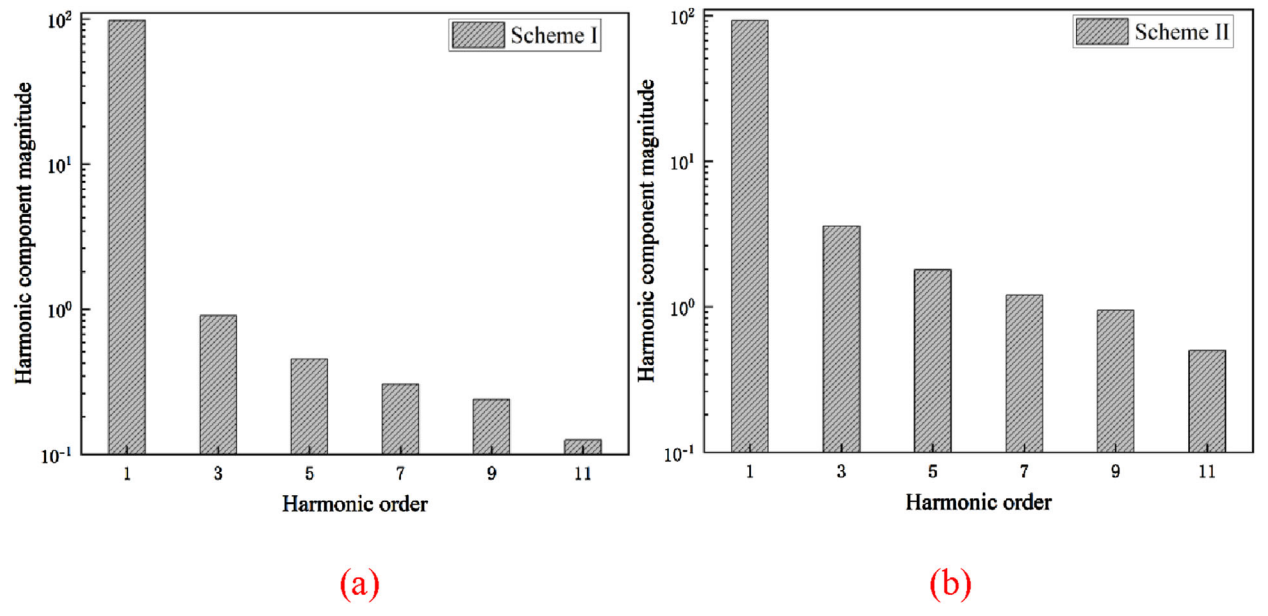

FIGURE 2
(a) Harmonic content of the applied voltage for Scheme 1; **(b)** Harmonic content of the applied voltage for Scheme 2.

TABLE 1 Parameters of zinc oxide surge arresters.

Rated voltage	110 kV
Continuous operating voltage	94 kV
Temporary overvoltage	130 kV
DC reference voltage	180 kV
Nominal discharge current	10 kA

quantities under voltage harmonic interference and aging faults were investigated to evaluate the robustness of the fifth harmonic against voltage harmonics and its effectiveness and reliability for aging monitoring. A monitoring and positioning scheme is also proposed. This methodology is specifically designed for aging monitoring and fault localization in zinc oxide surge arresters, enabling real-time degradation assessment and facilitating cost-effective operation and maintenance through predictive condition-based strategies.

2 Construction of the aging experimental platform for zinc oxide surge arresters

In the experiment, a variable low-voltage power supply of 0–240 V was employed. Two experimental schemes were designed. In Scheme I, a pure sinusoidal voltage was applied. But during experimental validation, the inherent nonlinearities of zinc oxide surge arresters and power transformers introduced harmonic distortions. Post-FFT analysis revealed a measured THD of 1.26%, with harmonic voltage components quantified as follows: third harmonic (V_{3rd}) at 0.907%, fifth harmonic (V_{5th}) at 0.454%, seventh harmonic (V_{7th}) at 0.305%, ninth harmonic (V_{9th}) at 0.239%, and eleventh harmonic (V_{11th}) at 0.126%,as shown in Figure 2a. In Scheme II, a voltage with a total harmonic distortion of 5% was applied to simulate the harmonic impact in power grids. The harmonic contents of the applied voltage included 3.6% third harmonic (V_{3rd}), 1.8% fifth harmonic (V_{5th}), 1.21% seventh harmonic (V_{7th}), 0.95% ninth harmonic (V_{9th}), and 0.5% eleventh harmonic (V_{11th}), as shown in Figure 2b.

TABLE 2 Parameters of transformer.

Voltage rating	240 V/150 kV
Rated Current	1 A
Frequency	50 Hz
Rated Power	150 kVA

Two zinc oxide surge arresters were selected for the experiment: one in a normal condition and the other in a severely aged and faulty condition. The normal condition refers to pristine, unused arresters post-manufacturing, while the aged condition corresponds to units that have been in continuous operation at Yancheng Substation, Jiangsu Province for a decade. The parameters of the arresters are listed in Table 1. An experimental circuit was constructed using a variable low-voltage power supply, voltage regulator, transformer, capacitive voltage divider, and high-precision current sensor, as shown in Figure 3, The capacitive voltage divider (FLDFR-150 kV) serves as a critical component for measuring the applied voltage. The accompanying display meter can display the magnitude and waveform of this voltage and transmit the waveform to a computer for FFT analysis to validate harmonic injection levels, and the value of the protective resistor is 10 kΩ. The arresters were subjected to voltages ranging from 70 to 120 kV using the variable low-voltage power supply and a step-up transformer, the parameters of the transformer are listed in Table 2. The applied voltage was monitored using a capacitive voltage divider, and its harmonic components were obtained using the FFT algorithm. The total leakage current was extracted using a high-precision current sensor (CM1A H00), and measure the total leakage current using a high-speed oscilloscope (HDO6054).

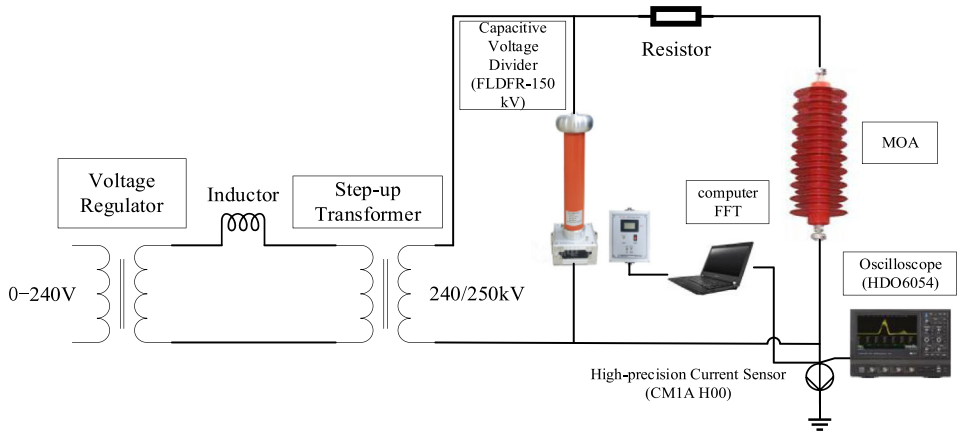

FIGURE 3
Experimental principle diagram.

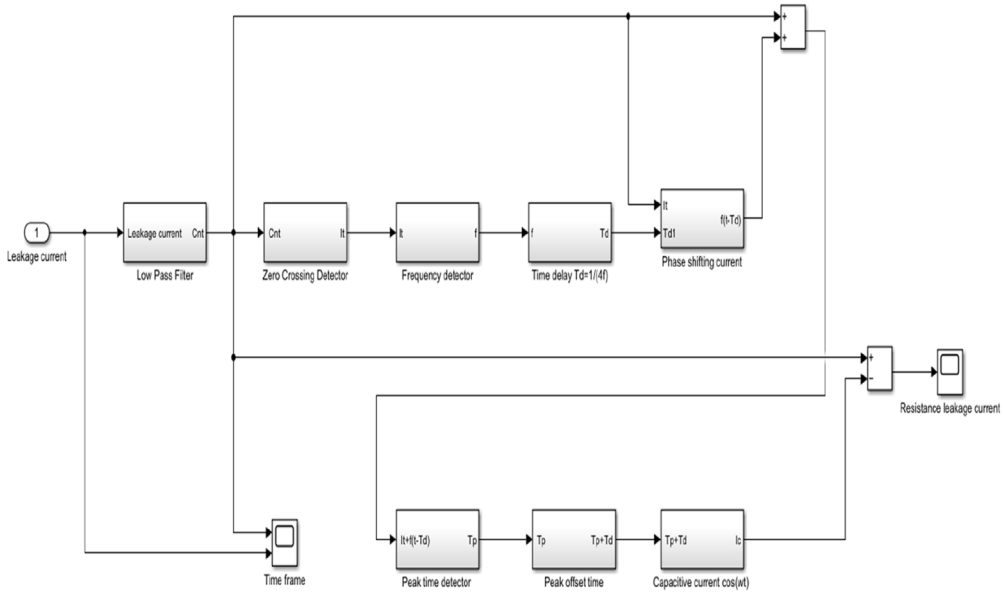

FIGURE 4
Simulink model of improved shift current method.

3 Harmonic feature extraction of the leakage current in zinc oxide surge arresters

The low-voltage power supply was adjusted to subject the arresters to voltages ranging from 70 to 120 kV through the step-up transformer. The input voltage and total leakage current were measured.

An improved displacement current method was employed to extract the resistive leakage current, as shown in the Simulink model in Figure 4. A zero-crossing detector was used to determine the phase of the current waveform, and a frequency detector was used to determine the frequency of the total leakage current. A new waveform was obtained by introducing a quarter-cycle delay to the total leakage current waveform, which was then added to the original total leakage current waveform to generate a composite waveform. The peak time of the composite waveform and that of the capacitive current component were determined using a peak time detector. The capacitive current waveform was generated based on the known frequency, peak time, and peak value. The resistive leakage current (I_R) was ultimately extracted by subtracting the capacitive current component (I_C) from the total leakage current.

The FFT was used to determine the third harmonic (I_{R3rd}) and fifth harmonic (I_{R5th}) of the resistive leakage current. Experiments were conducted on both normal and aged arresters under the two schemes, and the total leakage current (I_T), resistive leakage current (I_R), and their harmonics (I_{R3rd} and I_{R5th}) were measured and recorded. The overall process is shown in Figure 5.

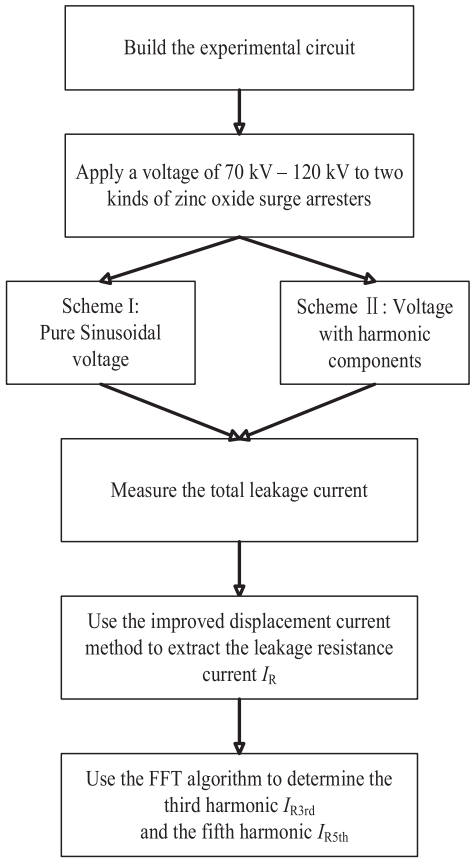

FIGURE 5
Overall flowchart of the harmonic extraction.

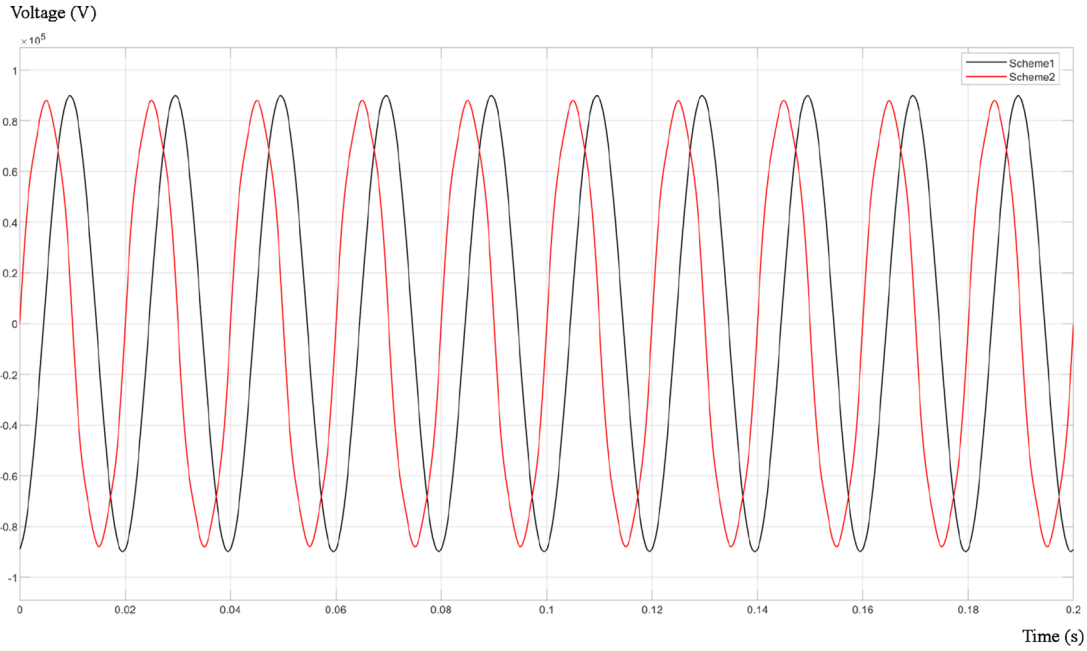

FIGURE 6
Applied voltage waveform.

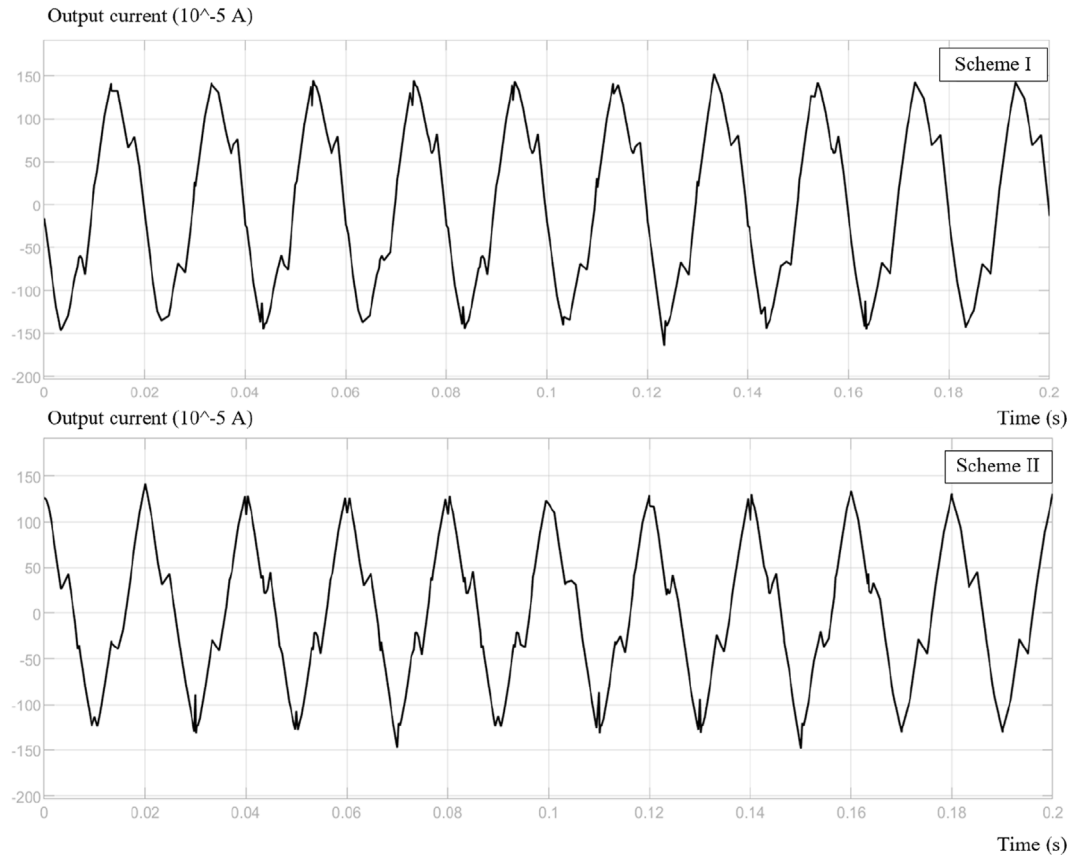

FIGURE 7
Total leakage current waveform.

TABLE 3 Total leakage current I_T for two schemes.

Applied voltage (kV)	Scheme I I_T (μA)	Scheme II I_T (μA)
70	826.9	827.4
80	946.8	948.5
90	1,115	1,117.2
94	1,168.5	1,171.4
98	1,237.4	1,241.8
100	1,289.8	1,295.7
110	1,475.6	1,484.9
120	2,395.2	2,425.5

TABLE 4 Resistive leakage current I_R for two schemes.

Applied voltage (kV)	Scheme I I_R (μA)	Scheme II I_R (μA)
70	320.2	320.5
80	389.9	390.7
90	543.5	544.8
94	595.3	597.5
98	641.2	643.9
100	706.0	712.2
110	870.4	881.9
120	2019.6	2061.7

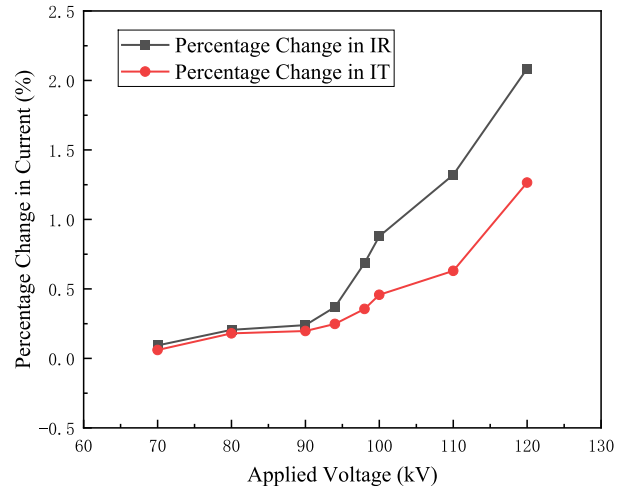

FIGURE 8
I_T and I_R percentage changes.

TABLE 5 Peak amplitudes of I_{R3rd} and I_{R5th}.

Applied voltage (kV)	I_{R3rd} peak amplitude (μA)		I_{R5th} peak amplitude (μA)	
	Scheme I	Scheme II	Scheme I	Scheme II
70	54.80	55.10	17.70	17.80
80	70.20	70.70	31.80	32.00
90	99.10	100.60	48.10	48.30
94	121.80	124.60	55.20	55.70
98	143.50	147.40	64.50	65.20
100	163.90	169.10	75.60	76.60
110	241.00	249.90	110.40	112.00
120	525.60	550.20	259.30	265.90

4 Characteristic analysis of I_{R5th}

4.1 Analysis of the anti-voltage harmonic interference capability of I_{R5th}

Under both Scheme I and Scheme II conditions, the arresters were subjected to voltages ranging from 70 to 120 kV, the voltage waveform is shown in Figure 6, Scheme I exhibits a standard sinusoidal voltage profile, while Scheme II demonstrates noticeable waveform distortion following the intentional introduction of harmonic components.

The current waveform of the transformer's high-voltage side output is shown in Figure 7. It is noteworthy that these waveforms directly represent the total leakage current of the surge arresters. Scheme I corresponds to the total leakage current under sinusoidal voltage conditions, whereas Scheme II reflects the leakage current under harmonic-distorted voltage conditions. The peak values of the total leakage current (I_T) were measured, as shown in Table 3. The resistive leakage current (I_R) was extracted from the total leakage current using the improved displacement current method, and its peak value was recorded, as shown in Table 3. It can be observed from Tables 3, 4 that, due to the addition of voltage harmonics in Scheme II, the total leakage current increased by 9.3 μA, and the resistive current increased by 11.5 μA under the rated voltage. The percentage changes in I_T and its I_R under Scheme II are shown in Figure 8. Under the rated voltage, the percentage increase in I_T was 0.63%, while the percentage increase in I_R was 1.32%. This indicates that the peak value of I_R increased more significantly than that of I_T due to voltage harmonics, as I_R is more sensitive to changes in voltage harmonics.

The peak amplitudes of I_{R3rd} and I_{R5th} were calculated using the FFT algorithm, as shown in Table 5. In Scheme I, the amplitude and nonlinearity of the resistive current varied with the applied voltage, and harmonic components were present in the resistive current. In Scheme II, the peaks of both I_{R3rd} and I_{R5th} increased

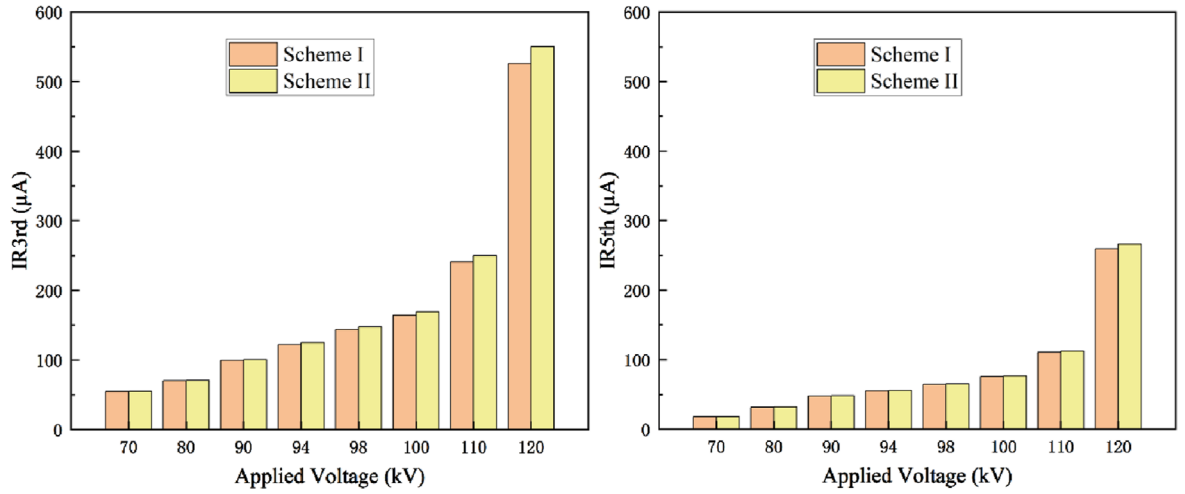

FIGURE 9
I_{R3rd} and I_{R5th} peak values of surge arresters in normal state.

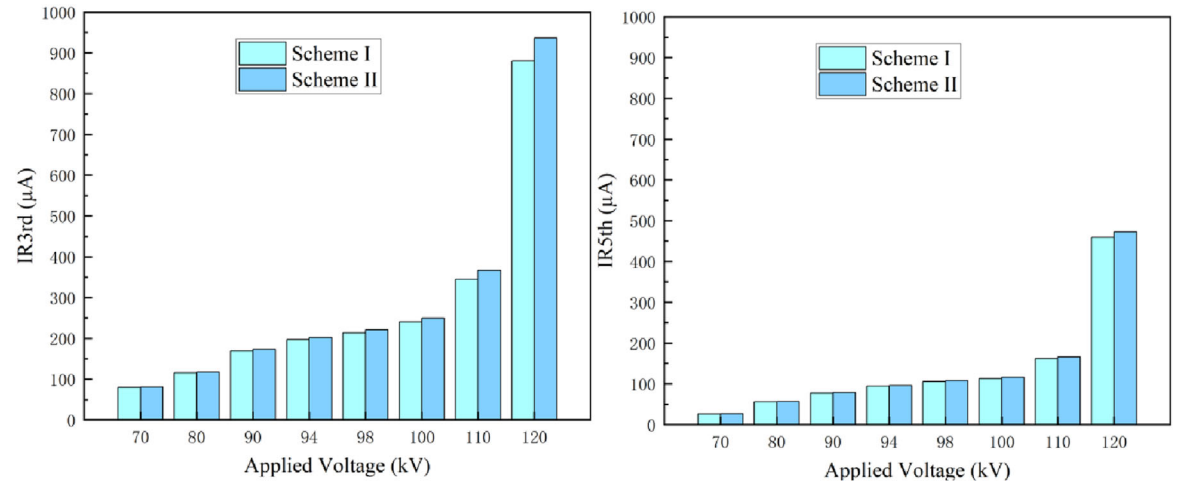

FIGURE 10
I_{R3rd} and I_{R5th} peak values of surge arresters in aging fault condition.

TABLE 6 Peak amplitudes of I_{R3rd} and I_{R5th}.

Applied voltage (kV)	I_{R3rd} peak amplitude (μA)		I_{R5th} peak amplitude (μA)	
	Scheme I	Scheme II	Scheme I	Scheme II
70	79.80	81.00	26.4	26.6
80	115.60	117.40	55.9	56.5
90	169.50	173.30	77.8	78.9
94	197.20	202.00	94.5	96.5
98	213.50	221.10	106.0	108.4
100	240.30	249.70	113.3	115.9
110	345.00	366.40	162.1	165.9
120	880.10	936.50	458.9	472.2

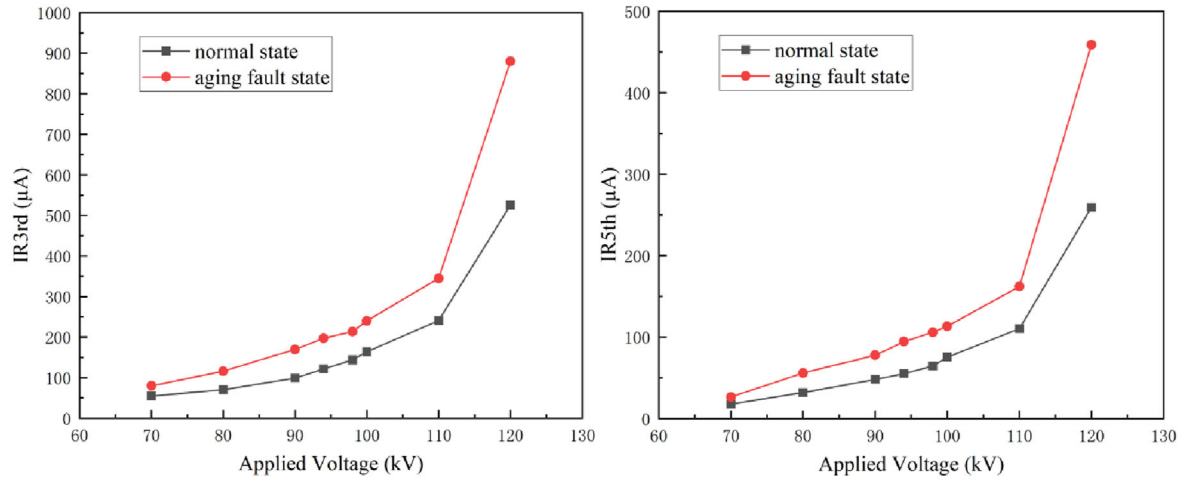

FIGURE 11
I_{R3rd} and I_{R5th} peak values in normal and aging fault conditions.

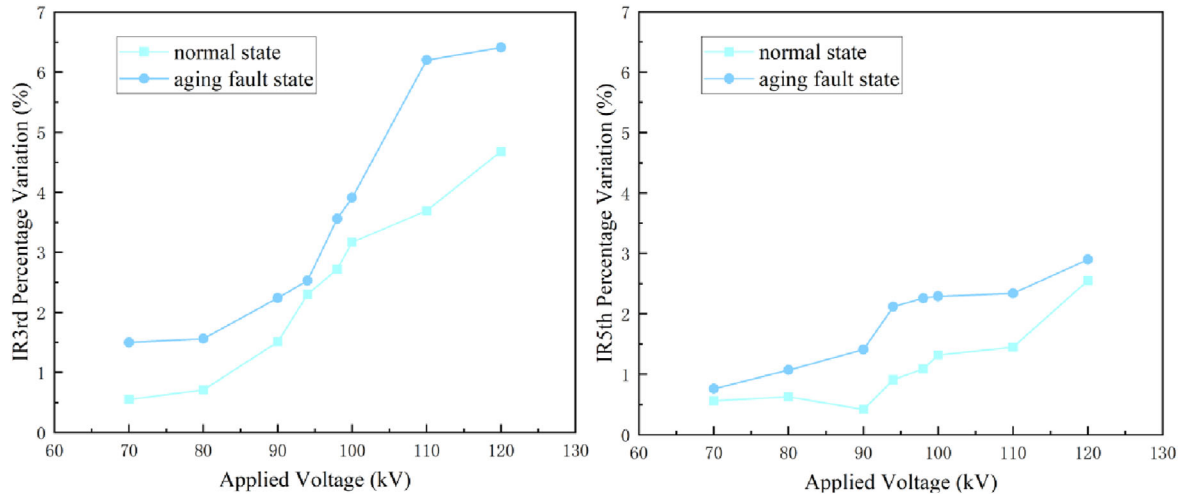

FIGURE 12
Percentage changes in I_{R3rd} and I_{R5th} in normal and aging fault conditions under harmonic interference.

TABLE 7 Data analysis of normal and aging fault conditions under harmonic interference.

Condition of arresters	I_{R3rd} percentage variation	I_{R5th} percentage variation	Percentage ratio
Normal condition	3.69	1.45	2.55
Aging fault condition	6.20	2.34	2.65

TABLE 8 Harmonic sensitivity analysis.

Feature parameter category	Harmonic sensitivity S
Total leakage current I_T	0.1793
I_{R3rd}	0.5157
I_{R5th}	0.1356

TABLE 9 I_{R5th} threshold judgment criteria for aging faults of zinc oxide surge arresters.

Applied voltage	I_{R5th}
90 kV < U ≤ 98 kV	>75 μA
98 kV < U ≤ 110 kV	>110 μA
110 kV < U	>300 μA

with the introduction of voltage harmonics. Under the rated voltage, the increases were 10.7 μA and 2.9 μA, respectively. When the percentage weight of V_{3rd} was nearly twice that of V_{5th}, the increase in the I_{R3rd} peak was 3.7 times that of I_{R5th}. This indicates that the

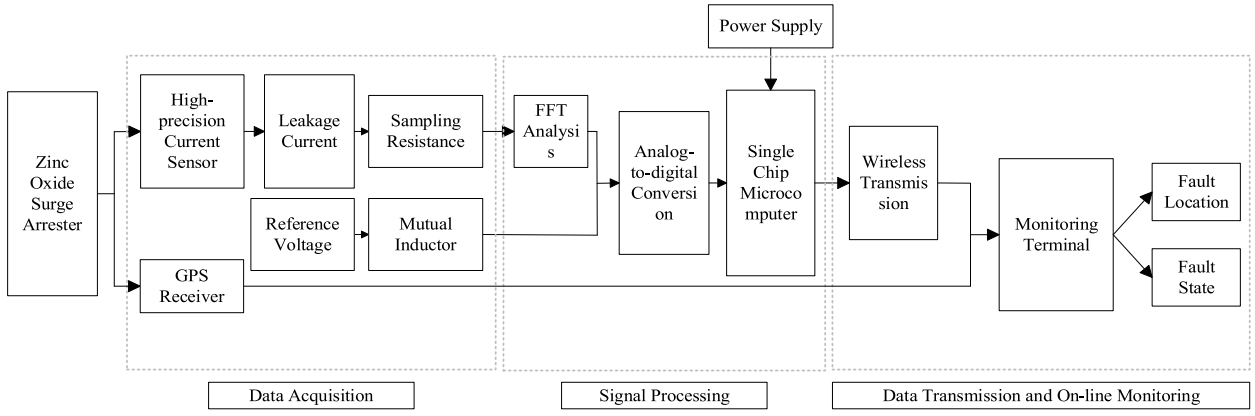

FIGURE 13
Schematic diagram of monitoring and positioning method for zinc oxide surge arresters.

increase in I_{R3rd} due to V_{3rd} is more significant than the increase in I_{R5th} due to V_{5th}.

4.2 Analysis of the effectiveness of I_{R5th} for aging monitoring

Under both Scheme I and Scheme II conditions, the applied voltage was different, and the I_{R3rd} and I_{R5th} of both normal and severely aged arresters were measured and calculated, as shown in Figures 9, 10, and the data for Figure 9 is shown in Table 5, and the data for Figure 10 is shown in Table 6. Under voltage harmonic interference, both current harmonics increased, but the change in I_{R3rd} was significant, while I_{R5th} remained relatively stable.

Comparing the data obtained in Scheme I, as shown in Figure 11, it is evident that both I_{R3rd} and I_{R5th} increased for the aged arresters compared to the normal condition, indicating that both harmonics can serve as indicators of aging and fault condition in zinc oxide surge arresters.

The percentage changes in the peaks of I_{R3rd} and I_{R5th} under harmonic interference were calculated for both types of arresters, as shown in Figure 12; Table 7. The percentage increase was more prominent in I_{R3rd} than in I_{R5th}. Although the percentage weight of V_{3rd} was nearly twice that of V_{5th} in Scheme II, the increase in the peak of I_{R3rd} was 2.55 and 2.65 times higher than that of I_{R5th} for the normal and aged arresters, respectively, under the rated voltage. This indicates that the impact of V_{3rd} on the peak of I_{R3rd} is greater than that of V_{5th} on the peak of I_{R5th}. This is attributed to the nonlinearity of zinc oxide surge arresters, leading to a more significant increase in I_{R3rd}. Additionally, the percentage increase in the aged arresters was higher than that in the normal arresters, validating the monitoring effectiveness of I_{R5th}. Therefore, it can replace I_{R3rd} as a new monitoring indicator.

4.3 Sensitivity analysis of I_{R5th} harmonics

In Scheme I, the peaks of I_{R3rd} and I_{R5th} were extracted independently of voltage harmonics. Therefore, the changes in the peaks of I_{R3rd} and I_{R5th} were compared by changing the magnitude of the applied voltage to verify the potential of I_{R5th} as a standard for aging fault assessment in zinc oxide surge arresters.

In Scheme II, the peaks of I_{R3rd} and I_{R5th} were influenced by voltage harmonics. The changes in the peaks of I_{R3rd} and I_{R5th} under the influence of V_{3rd} and V_{5th} were analyzed, and the percentage changes in the characteristic quantities were calculated and normalized by the percentage changes in the voltage harmonics. The average values were used to derive the sensitivity S expression:

$$S = \frac{1}{N-1}\sum_{i=1}^{N-1}\frac{[t_z(i+1)-t_z(i)]/t_z(i)}{[u_x(i+1)-u_x(i)]/u_x(i)} \quad (1)$$

Using Equation 1, the harmonic sensitivity S of the total leakage current I_T, I_{R3rd}, and I_{R5th} was calculated, as shown in Table 8. The results indicate that the harmonic sensitivity of I_{R5th} is lower than that of the other characteristic quantities. This suggests that, under voltage conditions with total harmonic interference, the value of I_{R5th} is less affected and provides high reliability for monitoring both the normal and aging fault conditions of arresters.

5 Aging monitoring and fault positioning for zinc oxide surge arresters

Based on the relationship between the resistive current harmonics (I_{R3rd} and I_{R5th}) and the applied voltage, threshold values for identifying the aging fault conditions of zinc oxide surge arresters were established, as shown in Table 9. The data provenance has been explicitly substantiated through statistical derivation from extensive experimental measurements, which systematically validates the threshold robustness.

I_{R5th} is proposed as a new indicator for fault diagnosis of arresters. The leakage current of the zinc oxide surge arresters is detected using a zero-flux high-precision current sensor. After FFT analysis and analog-to-digital signal processing, the data can be transmitted wirelessly for online monitoring. When the monitored value of I_{R5th} exceeds the aforementioned threshold, an alert is

triggered. Combined with a GPS positioning system, the location of the faulty arresters can be accurately obtained. The principle of the monitoring and positioning method is shown in Figure 13.

6 Conclusion

This study proposes a novel method for aging monitoring and fault positioning for zinc oxide surge arresters based on the fifth harmonic of the resistive leakage current (I_{R5th}). Initially, an aging experimental platform was established for zinc oxide surge arresters, and experiments were conducted with a voltage harmonic control group. Subsequently, the leakage current harmonic characteristics were extracted using an improved displacement current method and fast Fourier transform algorithm. The characteristics of I_{R5th} were analyzed through the percentage change in the feature and harmonic sensitivity analysis. Finally, by integrating high-precision current sensor technology with GPS positioning, a principle method for applying I_{R5th} to the fault monitoring and positioning for zinc oxide surge arresters was proposed. The following conclusions can be drawn:

- Under voltage harmonic interference, when the percentage weight of V_{3rd} is nearly twice as that of V_{5th}, the peak increase in I_{R3rd} is 3.7 times that of I_{R5th}, indicating that I_{R5th} has a stronger resistance to voltage harmonic interference.
- I_{R5th} exhibits similar sensitivity to aging faults as I_{R3rd}. However, under aging fault conditions, the percentage change in and harmonic sensitivity of I_{R5th} are lower than those of I_{R3rd}, showing improved data reliability. Therefore, I_{R5th} is more suitable for aging monitoring and fault positioning for zinc oxide surge arresters.

Data availability statement

The raw data supporting the conclusions of this article will be made available by the authors, without undue reservation.

Author contributions

YL: Writing – original draft, Writing – review and editing. ZX: Writing – original draft, Writing – review and editing. JG: Writing – original draft, Writing – review and editing. CZ: Writing – original draft, Writing – review and editing. JL: Writing – original draft, Writing – review and editing. XX: Writing – original draft, Writing – review and editing. JS: Writing – original draft, Writing – review and editing.

Funding

The author(s) declare that financial support was received for the research and/or publication of this article.

Conflict of interest

Authors YL, ZX, JG, CZ, JL, XX, and JS were employed by State Grid Jiangsu Electric Power Research Institute Co., Ltd.

This work was supported by the Project of State Grid Jiangsu Electric Power Co., Ltd. Science and Technology Funding in China (J2024068). The funder had the following involvement in the study: In terms of research design, the funder provided necessary space for experimental equipment, and during the paper writing phase, the funder offered necessary revision suggestions.

Generative AI statement

The authors declare that no Generative AI was used in the creation of this manuscript.

Publisher's note

References

1. Andrade AF, Costa EG, Fernandes JMB, Alves HM, Amorim Filho CR. Thermal behaviour analysis in a porcelain-housed ZnO surge arrester by computer simulations and thermography. *High Voltage* (2019) 4(3):173–7. doi:10.1049/hve.2019.0048

2. Kumar U, Mogaveera V. Voltage distribution studies on ZnO arresters. *IEE Proceedings-Generation, Transm Distribution* (2002) 149(04):457–62. doi:10.1049/ip-gtd:20020346

3. Wanderley Neto ET, Guedes da Costa E, Trajano de Souza R, Tavares de Macedo EC, de Albuquerque Maia MJ. Monitoring and diagnosis of ZnO arresters. *IEEE Latin America Trans* (2006) 4(3):170–6. doi:10.1109/tla.2006.4472110

4. Munir A, Abdul-Malek Z, Arshad RN. Resistive component extraction of leakage current in metal oxide surge arrester: a hybrid method. *Measurement* (2020) 173:108588. doi:10.1016/j.measurement.2020.108588

5. Das AK, Dey D, Chatterjee B, Dalai S. A transfer learning approach to sense the degree of surface pollution for metal oxide surge arrester employing infrared thermal imaging. *IEEE Sensors J* (2021) 21(15):16961–8. doi:10.1109/jsen.2021.3079570

6. Xu ZN, Zhao LJ, Ding A, Lu F. A current orthogonality method to extract resistive leakage current of MOSA. *IEEE Trans Power Deliv* (2013) 28(1):93–101. doi:10.1109/tpwrd.2012.2221145

7. Khavari AH, Munir A, Abdul-Malek Z. Circuit-based method for extracting the resistive leakage current of metal oxide surge arresters. *Bull Electr Eng Inform* (2020) 9(6):2213–21.

8. Schei A. Diagnostics techniques for surge arresters with main reference to online measurement of resistive leakage current of metal-oxide arresters. In: *International conference on large high voltage electric systems (CIGR´ E 2000)* (2000). p. 1–10.

9. Zhang J, Han Y, Li L, Deng J, Luo X, Meng Y, et al. Study on the unipolar impulse aging of ZnO varistors and their condition monitoring methods based on the basic and even-order harmonics of the leakage current resistive

component. *IEEE Trans Power Deliv* (2022) 37(6):4888–98. doi:10.1109/tpwrd.2022.3162203

10. Ji S, Yang L, Li Y, Zhang W, Wang X, Peng J, et al. Capacitive current compensation method for online monitoring of zinc oxide surge arresters. *High Voltage Eng* (2000) 04:16–8. doi:10.13336/j.1003-6520.hve.2000.04.007

11. Lundquist J, Stenstrom L, Schei A, Hansen B. New method for measurement of the resistive leakage currents of metal-oxide surge arresters in service. *IEEE Trans Power Deliv* (1990) 5:1811–22. doi:10.1109/61.103677

12. Doorsamy W, Bokoro P. Online monitoring of metal-oxide surge arresters using improved equivalent model with evolutionary optimisation algorithm. In: *2017 IEEE 26th international symposium on*. IEEE: Industrial Electronics ISIE (2017). p. 135–9.

13. Yamada T, Narita T, Shioda T, Okabe S, Zaima E. Observation and analysis of lightning surges at substations connected with UHV designed transmission lines. *IEEE Trans Power Deliv* (2000) 15(2):675–83. doi:10.1109/61.853004

14. Lira GRS, Barbosa VRN, Brito VS, Costa EG, Amorim Filho CRC, Maia MJA, et al. Methodology to evaluate the performance of metal-oxide surge arresters monitoring techniques based on the resistive leakage current. In: *Simposio Brasileiro de Sistemas Eletricos (SBSE)*. IEEE (2018). p. 1–6.

15. Fu Z, Wang J, Bretas A, Ou Y, Zhou G. Measurement method for resistive current components of metal oxide surge arresters in service. *IEEE Trans Power Deliv* (2017) 33:2246–53. doi:10.1109/TPWRD.2017.2776955

16. Novizon N, Malek Z, Bashir N, Asilah N. Thermal image and leakage current diagnostic as a tool for testing and condition monitoring of ZnO surge arrester. *Jurnal Teknologi* (2013) 64. doi:10.11113/jt.v64.2096

17. Zhang H, Wang R, Yu H. Online monitoring system of metal oxide arresters based on multi-layer support vector machine. *Insulators and Surge Arresters* (2020) 01:59–65. doi:10.16188/j.isa.1003-8337.2020.01.010

18. Mokhtari K, Mirzaie M, Shahabi M. Leakage current analysis of polymer and porcelain housed metal oxide surge arresters in humid ambient conditions. *Iranian J Electr and Electron Eng* (2015) 11(1):79.

19. Munir A, Abdul-Malek Z. Ageing detection of metal oxide surge arresters using fifth harmonic resistive current. In: *2020 IEEE international conference on power and energy (PECon)*. IEEE (2020). p. 382–5.

20. Wang L, Zuo Z, Wu C, Huang J, Qian Q. Analysis of the measurement principle of lightning arrester leakage current and development of built-in monitoring device. *High Voltage Apparatus* (2024) 60(08):174–82. doi:10.13296/j.1001-1609.hva.2024.08.021

21. Qi Q, Shi Y, Xu L, et al. Research on leakage current signal denoising algorithm of arre basedster on improved SSA. *J Wuhan Univ Technology* (2021) 43(06):76–82.

22. Khodsuz M, Mirzaie M. Evaluation of ultraviolet ageing, pollution and varistor degradation effects on harmonic contents of surge arresters leakage current. *IET Sci Meas and Technology* (2015) 9(8):979–86. doi:10.1049/iet-smt.2014.0372